BLOCK-BASED COLOR CONSTANCY: THE DEVIATION OF SALIENT PIXELS

Oguzhan Ulucan, Diclehan Ulucan, Marc Ebner

Institut für Mathematik und Informatik, Universität Greifswald, Greifswald, Germany
{oguzhan.ulucan, diclehan.karakaya, marc.ebner}@uni-greifswald.de

ABSTRACT

We recently proposed a color constancy method based on the observations that the human visual system might be *"discounting the illuminant"* by using space-average color and the highest luminance patches. Based on these observations, our algorithm relies on two assumptions: *(i)* there are several bright pixels in the scene, and *(ii)* the world is gray, on average. The main idea of the algorithm is to estimate the illuminant by finding the deviation of the brightest pixels from the gray value. During experiments, we observed that some pixels decrease the performance of the method. In this work, the algorithm is modified to eliminate the impact of these pixels. According to the comprehensive experiments, the proposed method surpasses several existing approaches on two color constancy benchmarks. Also, we show that the performance of some existing color constancy algorithms can be increased by using a block-based approach and salient pixels.

Index Terms—
Color Constancy, Illumination Estimation, White Balance

1. INTRODUCTION

The human visual system unconsciously perceives the true colors of objects in a scene regardless of the illumination conditions [1]. For instance, the human visual system perceives a white wall under a blue light source as white. However, when this scene is captured with a camera, due to the interaction between the sensitivity of the camera sensors and the light source of the scene, the wall in the image will be captured as blue. Correcting this color cast by removing the effects of the global illumination in the scene requires further computations. The field investigating the ways of discounting the illuminant is called *computational color constancy*, and it has significant importance in both digital photography and higher-level computer vision tasks such as object classification and image dehazing, which are utilized in several applications, i.e. robotics and security systems [2].

The image captured by a digital camera (with spatially varying illumination) can be formulated as

$$I_i(x, y) = \int_w R(x, y, \lambda) L(x, y, \lambda) S_i(\lambda) d\lambda \tag{1}$$

where, $I_i(x, y)$ is the measured signal at spatial location (x, y), $R(x, y, \lambda)$ is the reflectance of the surface, $L(x, y, \lambda)$ is the wavelength distribution of the light source, $S_i(\lambda)$ is the response function of the camera's color sensor with $i \in \{\text{red, green, blue}\}$, and λ is the wavelength of the visible spectrum w.

The aim of color constancy is to obtain a canonical image from the input image I by discounting the effects of the color vector of the light source L. However, estimating the color of the light source is an under-constrained problem, since both L and S are unknown. Therefore, many studies relax this problem by assuming the color sensors' responses are narrow-band and a global light source is illuminating the scene [2]. In this case, the image is obtained from the element-wise product of the reflectance of the surface R and the global light source L as follows

$$I(x, y) = R(x, y) \cdot L. \tag{2}$$

The field of color constancy has been extensively studied for more than four decades, and many color constancy algorithms have been introduced in the literature. Well-known methods, the white-patch Retinex [3] and the gray world [4], are based on the biological findings of the human visual system since the human visual system might be discounting the illuminant of the scene based on the highest luminance patch, and local space-average color [5]. While the white-patch Retinex algorithm finds the estimates of the light source by taking the maximum responses of the image channels separately, the gray world algorithm estimates the illuminant by averaging pixels of each channel independently. Due to their simplicity and effectiveness, most of the color constancy algorithms are built upon these two studies. For instance, the shades of gray algorithm [6] assumes that the mean of pixels raised to a certain power is gray. The gray-edge algorithm [7] and weighted gray-edge method [8] point out that the gradient features of the image are useful cues for estimating the illuminant. The mean-shifted gray pixel algorithm [9] transforms the task of illumination estimation into gray pixel detection. The illumination of the scene is estimated via mean-shift clustering based on the statistical properties of the color-biased image's gray pixels. The color constancy algorithm based on principal component analysis (PCA) [10] estimates the color vector of the light source by only considering the informative pixels, which have the largest gradient in the data matrix rather than using all the pixels in the scene. The local surface reflectance statistics [11] is based on the linear image formation model and relies on biological findings about the feed-back modulation mechanism in the eye. The biologically inspired method of Gao *et al.* [12] estimates the illuminant of the scene by using the responses of the double opponent cells in LMS space, where L, M and S correspond to the response of the cone types of the human eye.

Not only traditional approaches but also learning-based algorithms exist in the field of color constancy [13, 14, 15, 16, 17, 18]. These methods mostly surpass the traditional approaches on well-known benchmarks. Since these datasets are mostly captured with cameras, whose sensor response functions are similar, the algorithms, which are trained on these datasets face an inevitable challenge when they need to correct images with unique statistical distributions and/or images captured with devices with unknown hardware specifications [19, 20]. However, this is not a problem for traditional color constancy algorithms. Thereupon, we recently proposed a simple yet effective, learning-free color constancy method based on the

observations that the human visual system might be discounting the illuminant by using space-average color and the highest luminance patches in the scene [19]. The patch-based algorithm relies on two assumptions: *(i)* there are several bright pixels in the scene, *(ii)* on average, the world is gray. If the scene is gray on average, the deviation of the highest luminance pixels from a gray value should be caused by external effects, and this deviation should be in the direction of the global light source. During experiments, it is observed that not every pixel in a patch is informative to estimate the color vector of the global illuminant, for instance, the contribution of the patches containing dominant sky regions should be decreased. In this work, the algorithm is modified by only considering the pixels, which are closest to white to reduce the impact of the non-informative patches.

This paper is organized as follows. The proposed color constancy method and its modification are detailed in Sec. 2. Comprehensive experimental results are presented and discussed in Sec. 3, and a brief summary and possible future directions are given in Sec. 4.

2. PROPOSED METHOD

Since it was coined by Monge in 1789, color constancy has been intensively studied [21]. For more than four decades numerous color constancy methods are developed to find a solution to the ill-posed nature of color constancy. It is not surprising that the well-known solutions for discounting the illumination are based on the biological findings of the human visual system since one of the objectives in this domain is to understand how the brain arrives at the color constant descriptor of the scene [22]. Thereupon, we recently proposed a computational color constancy method based on the observations that the human visual system might be arriving at the color constant descriptor of the scene by using space-average color and highest luminance patch of the scene [5]. We assumed that the color constant descriptor of the scene can be simply obtained by considering that; *(i)* there is at least one bright pixel in the scene and *(ii)* on average, the world is achromatic. The main idea of the algorithm is that the deviation of the brightest pixels from the achromatic value should be caused by the global light source. Hence, finding this deviation will result in estimating the color vector of the light source, and subsequently arriving at the color constant descriptor of the scene. In this section, the steps of the proposed method and the modifications are detailed.

The proposed method can take both linear-raw and sRGB images as input. In case the algorithm is applied to an sRGB image, linearization should be applied in order to obtain a linear relationship between the image elements. Also, since it is known that the darkest and brightest pixels are negatively affecting the performance of the color constancy studies, corresponding pixels are clipped to reduce possible noise, i.e. the darkest and brightest pixels in the image are not considered in the calculations. Afterwards, the image is divided into non-overlapping patches $\{I_p\}_{p=1}^{n}$, where n is the number of non-overlapping blocks, which is the only fixed parameter of the proposed method. The determination of n is discussed in Sec. 3.

Since the algorithm is built upon the assumptions of the white-patch Retinex and gray world method, it is assumed that for each patch I_p, there exists at least one bright pixel and a unique achromatic value, which are the most informative elements to find the illumination of I_p. The brightest pixel values (per channel) of I_p can be simply determined by taking the maximum response of each channel. These maximum intensity values form the informative intensity vector $I_{p,max}$, where $I_{p,max} = [R_{p,max}, G_{p,max}, B_{p,max}]$. The achromatic value μ_p can be calculated by simply taking the mean of all pixels in the image, but it is observed that using a single fixed achromatic value for all I_p negatively affects the performance of the algorithm. This is not surprising, since the local surface orientations of the scene vary throughout the image, in other words, a unique achromatic value exists for each distinct I_p, and it can be computed by taking the mean μ_p of pixels over all channels within the patch of interest. After determining both of these informative elements, the illumination estimate of each I_p can be found by considering the second assumption of the proposed method, the world is gray on average. It is important to note here that, if the scene is achromatic on average, the summation of the intensity values of $I_{p,max}$ is assumed to be gray. But, if there is a color cast in the scene, it should cause a deviation from the gray world. For each distinct I_p, this shift away can be found by computing a scaling vector $\mathbf{C}_p = [c_r, c_g, c_b]$, which scales the intensities of the $I_{p,max}$ such that they sum to a gray value μ_p as follows;

$$R_{p,max} \cdot c_r + G_{p,max} \cdot c_g + B_{p,max} \cdot c_b = \mu_p. \tag{3}$$

Consequently, the scaling vector $\mathbf{C}_p$ can be computed by solving the constrained optimization problem as follows;

$$\mathbf{C_p} = \arg\min_{\mathbf{C_p}} \left\| I_{p,max}\, \mathbf{C_p} - \mu_p \right\|_2 \quad with \quad \forall c \in \mathbf{C_p} : c \geq 0. \tag{4}$$

Since it is assumed that there is a single light source illuminating the scene, the color vector of the illumination is calculated by averaging every $\mathbf{C}_p$ as follows;

$$\mathbf{L_{est}} = \frac{1}{n} \sum_{p=1}^{n} \mathbf{C_p}. \tag{5}$$

Finally, the color constant descriptor of the scene is found by re-scaling the original image according to $\mathbf{L_{est}}$ by using Eqn. 2.

Note that not all elements of the patches are helpful in estimating the color vector of the light source. For instance, a patch containing a dominant sky region will bias the estimations for that I_p, hence it will decrease the performance of the algorithm (Fig. 2). Therefore, in this study, the proposed method is modified in order to overcome this problem with a simple yet effective approach. Instead of using all the pixels within the patch, only the salient pixels are considered to find the deviation from the gray world. These salient regions are obtained from the pixels, which are closest to white. The motivation for using only these image elements rather than all the pixels of an image can be explained by a simple example from digital photography [2]. Let us assume that an image of a room illuminated by blue light, which has white walls and contains colored objects is captured by a digital camera, whose white balance setting is disabled. Since the captured image is an integrated signal obtained from the response of the camera's color sensor functions and the scene illumination, every spatial location of the image has an undesirable color cast. In particular, the white walls will shift towards the color blue. The light source can be easily estimated from the white wall rather than the colored objects since the camera sensors will measure the white wall illuminated by blue light as blue. Hence, even if the scenes have very complicated color distributions, the color of the light vector can be approximated by using the pixels closest to white. These pixels can be easily found by assuming the world is gray on average. A temporary color vector of the light source L_{temp} can be estimated by taking the mean values of each color channel. Subsequently, a temporary white balanced image I_{temp} can be obtained by scaling the original image according to L_{temp} as in Eqn. 2. Then, the pixels closest to white can be determined by checking the angular error (explained in Sec. 3) between the pixels of I_{temp} and the white vector, $[1, 1, 1]$. Generally, the pixels having an angular error less than 5 are considered to be salient pixels, which are closest to white and only these pixels are considered in the proposed algorithm to estimate the global light source illuminating the scene.

Fig. 1. Examples images. First two images are from the INTEL-TAU and last two are from the RECommended ColorChecker dataset.

3. EXPERIMENTAL SETUP AND RESULTS

The proposed method is compared with the following statistical methods, white-patch Retinex [3], gray world [4], shades of gray [6], 1^{st} and 2^{nd} order gray-edge [7], weighted gray-edge [8], double-opponent cells based color constancy [12], PCA based color constancy [10], color constancy with local surface reflectance estimation [11], and mean-shifted gray pixels [9] which are all briefly explained in Section 1. Also, a comparison with the proposed method's initial version is provided. The codes for the algorithms are obtained from the official webpages of the authors and they are used in their default settings without any modification. The experiments are conducted on an Intel i7 CPU @ 2.7 GHz Quad-Core 16 GB RAM machine.

The algorithms are evaluated on the widely used color constancy benchmarks, INTEL-TAU [23] and Recommended ColorChecker [24] datasets. The INTEL-TAU dataset is one of the largest color constancy benchmarks containing a total of 7022 indoor and outdoor scenes captured with three different cameras, Canon 5DSR, Nikon D810, and Mobile Sony IMX135. The Recommended ColorChecker dataset is an updated version of the Gehler-Shi dataset [25]. It contains a total of 568 for indoor and outdoor images captured with two cameras, Canon 1D and Canon 5D. Both datasets contain images captured under one dominant light source to avoid mixed illumination conditions (Fig. 1). Also, the images in both these datasets have a linear response and their black level is calibrated. Another common feature of both datasets is that they are captured with cameras, whose camera sensitivities differ. Since it is important to compare color constancy algorithms with images, whose spectral distribution is unknown, in the experiments the images belonging to the same dataset are combined to create a single set, i.e. a camera-unknown set.

To statistically benchmark the performance of each method, the angular error, which is widely used in the field of color constancy is adopted. The angular error (ε) between the ground truth illuminant ($\mathbf{L}_{gt}$) and the estimated illuminant ($\mathbf{L}_{est}$) can be computed as follows;

$$\varepsilon(\mathbf{L}_{gt}, \mathbf{L}_{est}) = cos^{-1}\left(\frac{\mathbf{L}_{gt}\mathbf{L}_{est}}{\|\mathbf{L}_{gt}\|\|\mathbf{L}_{est}\|}\right). \quad (6)$$

The mean, the median, the mean of the best 25%, and the mean of the worst 25% of the angular error are reported in Table 1.

In the experiments, the proposed method is investigated thoroughly. The effects on the performance of using non-overlapping blocks and salient pixels not only for the proposed method but also for the algorithms on which the proposed method is built upon are investigated in detail. As seen in Table 1, it is clear that the performances of the white-patch Retinex and the gray world algorithms significantly increase when they are modified by using the non-overlapping blocks and salient pixels. Furthermore, to show the importance of dividing images into non-overlapping patches and choosing only the salient pixels to compute the color vector of the light source the proposed algorithm is compared with its different versions in the last four rows of Table 1. When the proposed algorithm is employed without dividing the image into blocks and without the consideration of the salient pixels, its performance tends to decrease significantly. As seen from the results, estimating the illuminant by dividing the image into blocks and considering only the salient pixels in the scene greatly improves the effectiveness of the algorithm. The reason behind this performance increase can be explained with the facts that *(i)* the statistical distributions of the scenes are not uniform throughout the image, but they change in local regions and *(ii)* not all pixels contain useful information. In other words, investigating the non-overlapping blocks independently allows us to give more importance to local regions, and pixels, which are non-informative, negatively affect the outcomes, hence they should be eliminated during processing (Fig. 2).

Fig. 2. The visual comparison of the proposed method with its initial version. (Left-to-right) Input image, initial version, proposed method, the ground truth, and the salient pixels. The angular error is provided on the bottom-right side of the image.

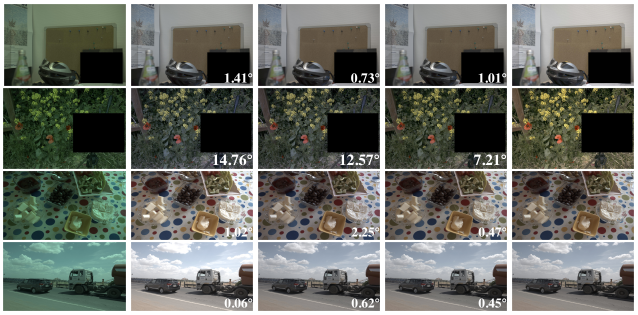

Fig. 3. Comparison of algorithms. (Left-to-right) Input image, the result of local surface reflectance estimation, mean shifted gray pixel, proposed method, and the ground truth image. The angular error of each method is provided on the bottom-right side of the image.

The proposed method outperforms the state-of-the-art in the experiments. The lowest mean angular error is achieved by the proposed method for both benchmarks. Moreover, the median of the angular error of the proposed method is lower than the mean of the angular error for both datasets, which indicates that the proposed algorithm produces outcomes closer to the best cases rather than the worst ones. Furthermore, as seen in Table 1, the mean of the best 25% of the angular error mostly does not significantly differ among algorithms compared to the mean of the worst 25% of the angular error. The performance gap among techniques increases considerably when the worst cases are taken into account, where the proposed algorithm clearly outperforms existing techniques on both benchmarks. This outcome is noteworthy since it is known that in color constancy studies, aside from the mean angular error, it is also important to decrease the mean of the worst 25% of the angular error [19].

In Fig. 3 the visual comparisons of the proposed method with the best-performing algorithms are provided for both indoor and outdoor scenes. The proposed method is able to produce images close to the

Table 1. Statistical results of the methods. For each metric the best result is highlighted.

	INTEL-TAU Camera-Unknown				RECommended ColorChecker Camera-Unknown			
	Mean	**Median**	**B-25%**	**W-25%**	**Mean**	**Median**	**B-25%**	**W-25%**
White-Patch Retinex	11.01	13.16	1.81	19.44	10.27	9.12	1.64	20.50
Gray World	4.91	3.88	0.96	10.60	4.74	3.61	0.97	10.44
Shades of Gray Edge	5.51	4.16	0.97	12.29	5.87	4.25	0.75	13.72
1^{st} order Gray Edge	6.10	4.23	0.96	14.27	6.42	3.84	0.94	15.83
2^{nd} order Gray Edge	6.41	4.50	1.04	14.73	6.94	4.41	1.07	16.53
Weighted Gray Edge	6.00	3.64	0.81	14.90	6.10	3.33	0.79	15.59
Double-Opponent Cells based Color Constancy	7.19	4.67	0.81	16.98	7.24	4.26	0.80	18.05
PCA based Color Constancy	4.47	3.03	0.69	10.64	4.11	**2.52**	0.53	10.19
Local Surface Reflectance Estimation	4.17	3.42	0.98	8.61	4.03	3.07	1.40	8.17
Mean Shifted Gray Pixels	3.57	**2.56**	0.64	8.24	3.81	2.96	0.77	8.35
White-Patch Retinex: Block-based with Salient Pixels	3.41	2.65	0.79	7.36	4.05	2.93	0.94	8.99
Gray World: Block-based with Salient Pixels	3.69	2.58	**0.63**	8.60	4.39	2.80	**0.52**	10.85
Proposed: Without Blocks and Salient Pixels	8.74	7.89	1.74	17.08	9.23	7.49	2.79	18.11
Proposed: Without Blocks and with Salient Pixels	5.92	4.11	1.04	13.72	6.44	4.73	1.55	14.06
Initial Version	4.29	3.61	1.20	8.53	3.82	3.17	1.46	7.38
Proposed	**3.37**	2.63	0.79	**7.25**	**3.48**	2.71	1.06	**7.35**

Table 2. Investigation of the kernel size of the non-overlapping blocks. The kernel size having the lowest mean angular error is selected.

	INTEL-TAU Random Set							RECommended ColorChecker Random Set						
	8×8	**16×16**	**32×32**	**64×64**	**128×128**	**300×300**	**600×600**	**8×8**	**16×16**	**32×32**	**64×64**	**128×128**	**300×300**	**600×600**
Mean Angular Error	3.759	3.747	3.733	3.729	**3.725**	3.733	3.783	3.630	3.603	3.571	3.542	3.518	**3.492**	3.607

ground truths, which coincides with its statistical results. However, if the statistical distribution throughout the image is uniform and the image does not contain any salient pixels, the performance of the algorithm tends to decrease. It is important to note that, this is a common problem for statistical-based color constancy algorithms.

As a final note, the size of the non-overlapping patches is the only fixed parameter of the proposed method as mentioned in Sec. 2. The investigation of this parameter is presented in Table 2 for both benchmarks. This parameter is determined experimentally by investigating the relationship between the mean angular error and different kernel sizes. In order to perform the experiments, a sub-set called *random set* is generated by randomly choosing images from the datasets. As seen in Table 2, the performance of the proposed algorithm increases when the input scene is divided into a sufficient number of non-overlapping patches. When the images are divided into 600×600 sized kernels only a small number of blocks is obtained, hence the performance is lower than desired. One reason for this performance decay might be that the surface orientations are not uniform throughout the image, but they differ in the local regions, and when a limited number of blocks are considered, the amount of information taken into account is reduced significantly. Therefore, when the number of blocks is increased, i.e. the kernel size is decreased, the proposed algorithm can take more distinct features into account, which positively affects its outcomes. However, it should be noted that if the kernel size is too small the performance of the algorithm tends to decrease. This is due to the fact that one of the assumptions the proposed algorithm is built upon is the gray world assumption, which is only valid when the image contains an adequate number of distinct colors, i.e. when the patches are too small the possibility of having uniform colored blocks increases. Consequently, selecting the number of blocks is an important step of the proposed algorithm, and this parameter mainly depends on the image resolution. For both color constancy benchmarks, different kernel sizes are selected, since the resolution of the images in the datasets varies. In the INTEL-TAU dataset, the resolution of the images is smaller than the resolution of the images in the RECommended ColorChecker dataset. Thus, the kernel sizes are selected as 128×128 and 300×300 for the INTEL-TAU and RECommended ColorChecker datasets, respectively.

4. CONCLUSION

Recently we have proposed a color constancy algorithm relying on the observations that the human visual system might be discounting the effects of the light source based on the highest luminance patch and space-average color. The strongest sides of the proposed algorithm are that it is a learning-free method and it has only one fixed parameter, which is the size of the non-overlapping patches. The algorithm first divides the image into non-overlapping blocks and then for each patch, the method finds the estimation of the light source by finding the deviation of the brightest pixels from the gray value. The estimate of the global light source is obtained by averaging the estimates of each patch. Since not all pixels in the patches carry informative features in estimating the color vector of the light source, for instance, the method has difficulty correcting scenes having a dominant sky region. In this work, this problem is overcome by considering only the patches containing the salient pixels, i.e. pixels closest to white. With this modification, the proposed method statistically outperforms the state-of-the-art algorithms on well-known color constancy benchmarks. Additionally, in this study, we showed that the performance of some color constancy algorithms can be easily improved by using a block-based approach and salient pixels. As future work, the algorithm will be modified for mixed illumination conditions.

5. REFERENCES

[1] S. Zeki, *A Vision of the Brain.*, Blackwell Science, 1993.

[2] M. Ebner, *Color Constancy, 1st ed.*, Wiley Publishing, 2007.

[3] E. H. Land, "The retinex theory of color vision," *Scientific Amer.*, vol. 237, pp. 108–129, 1977.

[4] G. Buchsbaum, "A spatial processor model for object colour perception," *J. Franklin Inst.*, vol. 310, pp. 1–26, 1980.

[5] M. Ebner, "A parallel algorithm for color constancy," *J. Parallel Distrib. Comput.*, vol. 64, pp. 79–88, 2004.

[6] G. D. Finlayson and E. Trezzi, "Shades of gray and colour constancy," in *Color and Imag. Conf.*, Scottsdale, AZ, USA, 2004, Society for Imaging Science and Technology, pp. 37–41.

[7] J. Van De Weijer, T. Gevers, and A. Gijsenij, "Edge-based color constancy," *IEEE Trans. Image Process.*, vol. 16, pp. 2207–2214, 2007.

[8] A. Gijsenij, T. Gevers, and J. Van De Weijer, "Physics-based edge evaluation for improved color constancy," in *Conf. Comput. Vision Pattern Recognit.*, Miami, FL, USA, 2009, IEEE, pp. 581–588.

[9] Y. Qian, S. Pertuz, J. Nikkanen, J.-K Kämäräinen, and J. Matas, "Revisiting gray pixel for statistical illumination estimation," *arXiv preprint arXiv:1803.08326*, 2018.

[10] D. Cheng, D. K. Prasad, and M. S. Brown, "Illuminant estimation for color constancy: Why spatial-domain methods work and the role of the color distribution," *J. Opt. Soc. America A*, vol. 31, pp. 1049–1058, 2014.

[11] S. Gao, W. Han, K. Yang, C. Li, and Y. Li, "Efficient color constancy with local surface reflectance statistics," in *Eur. Conf. Comput. Vision*, Zurich, Switzerland, 2014, Springer, pp. 158–173.

[12] S. Gao, K. Yang, C. Li, and Y. Li, "Color constancy using double-opponency," *IEEE Trans. Pattern Anal. Mach. Intell.*, vol. 37, pp. 1973–1985, 2015.

[13] M. Afifi, J. T. Barron, C. LeGendre, Y.-T. Tsai, and F. Bleibel, "Cross-camera convolutional color constancy," in *Int. Conf. Comput. Vision*, Montreal, QC, Canada, 2021, IEEE/CVF, pp. 1981–1990.

[14] M. Afifi and M. S. Brown, "Sensor-independent illumination estimation for DNN models," in *Brit. Mach. Vision Conf.*, Cardiff, UK, 2019, BMVA Press, pp. 12.1–12.13.

[15] M. Afifi and M. S. Brown, "Deep white-balance editing," in *Conf. Comput. Vision Pattern Recognit.*, Seattle, WA, USA, 2020, IEEE/CVF, pp. 1397–1406.

[16] M. Afifi, M. A. Brubaker, and M. S. Brown, "Auto white-balance correction for mixed-illuminant scenes," in *Winter Conf. Appl. Comput. Vision*, Waikoloa, HI, USA, 2022, IEEE/CVF, pp. 1210–1219.

[17] I. Domislović, D. Vršnak, M. Subašić, and S. Lončarić, "Onenet: Convolutional color constancy simplified," *Pattern Recognit. Letters*, vol. 159, pp. 31–37, 2022.

[18] F. Laakom, J. Raitoharju, A. Iosifidis, J. Nikkanen, and M. Gabbouj, "Color constancy convolutional autoencoder," in *Symp. Ser. Comput. Intell.*, Xiamen, China, 2019, IEEE, pp. 1085–1090.

[19] O. Ulucan, D. Ulucan, and M. Ebner, "Color constancy beyond standard illuminants," in *Int. Conf. Image Process.*, Bordeaux, France, 2022, IEEE, pp. 2826–2830.

[20] S. Gao, M. Zhang, C. Li, and Y. Li, "Improving color constancy by discounting the variation of camera spectral sensitivity," *J. Opt. Soc. America A*, vol. 34, pp. 1448–1462, 2017.

[21] O. Ulucan, D. Ulucan, and M. Ebner, "BIO-CC: Biologically inspired color constancy," in *Brit. Mach. Vision Conf.*, London, UK, 2022, BMVA Press.

[22] M. Ebner, "How does the brain arrive at a color constant descriptor?," in *Int. Symp. Brain Vision Artif. Intell.*, Naples, Italy, 2007, Springer, pp. 84–93.

[23] F. Laakom, J. Raitoharju, J. Nikkanen, A. Iosifidis, and M. Gabbouj, "Intel-tau: A color constancy dataset," *IEEE Access*, vol. 9, pp. 39560–39567, 2021.

[24] G. Hemrit, G. D. Finlayson, A. Gijsenij, P. Gehler, S. Bianco, B. Funt, M. Drew, and L. Shi, "Rehabilitating the colorchecker dataset for illuminant estimation," in *Color Imag. Conf.*, Vancouver, BC, Canada, 2018, Society for Imaging Science and Technology, pp. 350–353.

[25] P. V. Gehler, C. Rother, A. Blake, T. Minka, and T. Sharp, "Bayesian color constancy revisited," in *Conf. Comput. Vision Pattern Recognit.*, Anchorage, AK, USA, 2008, IEEE, pp. 1–8.